LA-UR-95-2685

BUCKLING AND COLLAPSE ANALYSIS OF AN UNDERGROUND DOUBLE-SHELL HIGH-LEVEL WASTE TANK SUBJECTED TO VACUUM LOADS

LA-UR-95-2685

June 1995

by

Edward A. Rodriguez
Rich F. Davidson

Engineering & Safety Analysis Group
Technology & Safety Assessment Division

LOS ALAMOS NATIONAL LABORATORY

TABLE OF CONTENTS

1.0 ABSTRACT

This paper presents an analysis to determine the buckling capacity and the collapse limit of the High-Level Waste (HLW) Tank 101-SY primary steel liner. The analysis considers the effects of vacuum pressure and additional dead weight of saltcake assumed to be adhered to the primary liner sidewall, at reduced tank waste levels. The stability conditions of the tank liner are of great concern at reduced tank levels, during normal operations when a vacuum condition exists. The reduced tank level concern is due to the lack of load-stiffening effect from hydrostatic pressure. Furthermore, sections of saltcake adhered to the sidewall, that extend inward, tend to impose a localized bending moment to the liner that induces premature collapse. Results show the buckling capacity of the tank as a function of waste level, with the lower-bound capacity of the empty tank at 1.7 psig.

2.0 INTRODUCTION

The bulk of underground double-shell waste tanks at the Hanford Site in Richland, Washington were designed in accordance with the rules of the ASME Code[1] to be capable of withstanding a maximum 6" H_2O vacuum (0.22 psig) minimum and 60" H_2O (positive) pressure (2.17 psig). Under normal operating conditions, the tank dome space will be subjected to about 2" H_2O vacuum pressure (0.07 psig), as stipulated in the Interim Safety Basis[2] and the Operating Specifications Document[3].

Recent analyses performed by WHC[4] show that under certain conditions, specifically decontamination operations using spray water wands, the dome pressure may reach 15" to 20" H_2O vacuum. Obviously, this condition has not been investigated since the tank design stipulates a maximum of 6" H_2O vacuum.

Coupled with this finding, there is a concern that waste retrieval activities may impose additional shell-liner stresses from the dead weight of (potential) saltcake adhered to the tank wall. It is not yet known, whether during retrieval activities, waste crust will remain adhered to the walls. The adhered saltcake may be extensive, based on videotape evidence of existing crust on tank walls around the inner periphery of the tank and knowledge of the crust shear strength. The saltcake may extend inward from the primary liner (i.e., cantilevered from the wall), further imposing an eccentric load on the shell, causing a localized bending moment and subsequent premature failure.

The structural stability of tank 101-SY will be investigated to determine the actual buckling capacity and collapse limit load under vacuum conditions plus the supposition of additional dead weight of saltcake on the tank wall. Lastly, the results are compared with WHC buckling analysis of a free-standing cylindrical shell.

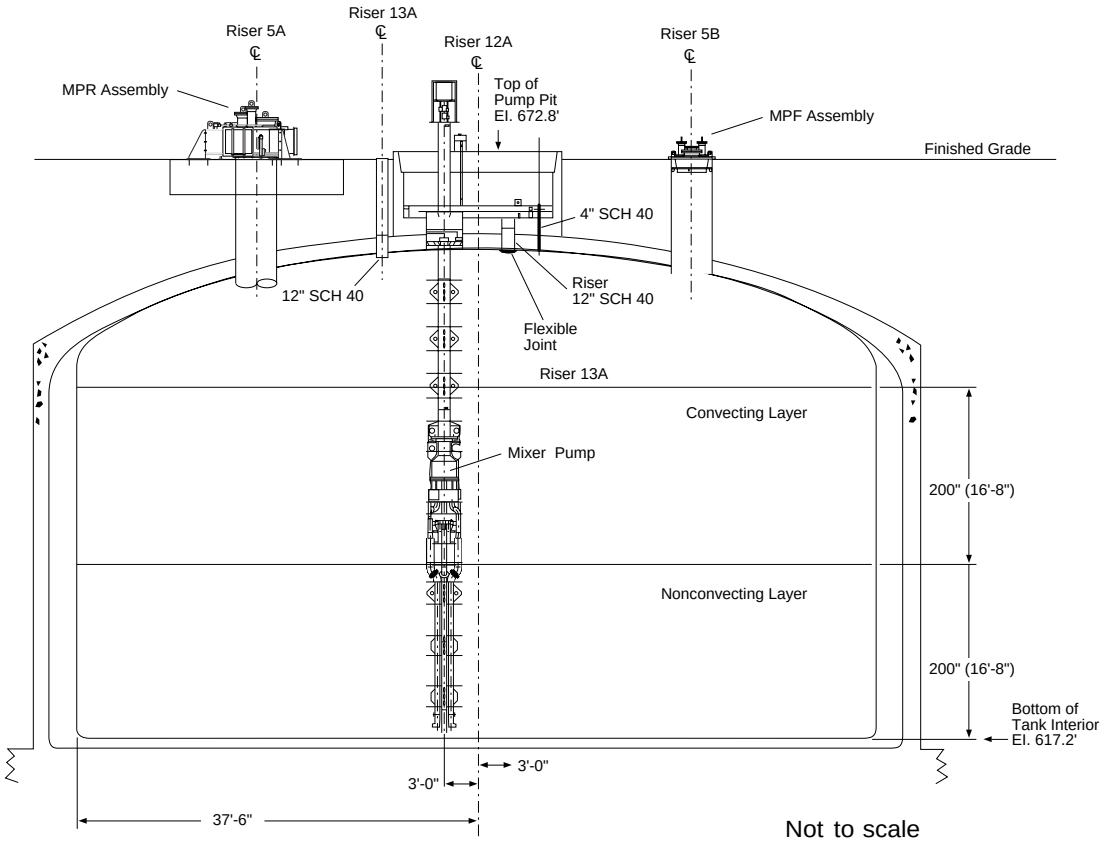

Fig. 2.1 - HLW Tank 101-SY cross-sectional view

3.0 ANALYTICAL METHODS AND ASSUMPTIONS

Three methods are used to assess the elastic stability and the elastic-plastic collapse of the primary steel liner. The first method is based on classical linear-elastic stability theory[5] for unstiffened cylindrical shells derived from elasticity theory. This method will also be compared against the design acceptance criteria of the ASME Code[1] to determine its safety margin from its original design.

The second method is an elastic buckling (eigenvalue) analysis of the tank primary liner structure. The eigenvalue buckling analysis is based on a 3-D finite element model representation of the tank primary liner structure performed with the ABAQUS code[6].

The third method is also based on a 3-D finite element model of the tank primary liner structure solving the geometric non-linear load-displacement characteristics. This is virtually a structural collapse analysis predicting the post-buckling behavior of the structure, and determining the bifurcation and limit loads. In many cases

where structures are “imperfection sensitive,” the actual collapse load may be significantly lower than the bifurcation load predicted by the eigenvalue buckling analysis.

This model, therefore, takes into consideration the load-stiffening effect of the hydrostatic pressure from the waste. The finite element analysis model, performed with the ABAQUS code[6], also takes into consideration the elastic and elastic-plastic behavior of the steel, large displacement formulation (non-linear geometric effects), and “follower-type” pressure loads in allowing the structure to reach a collapse load (or limit load). The collapse analysis monitors the load-deflection characteristic of the structure, whether in a stable or unstable condition (as shown in Fig. 2), as the internal vacuum pressure is incrementally applied.

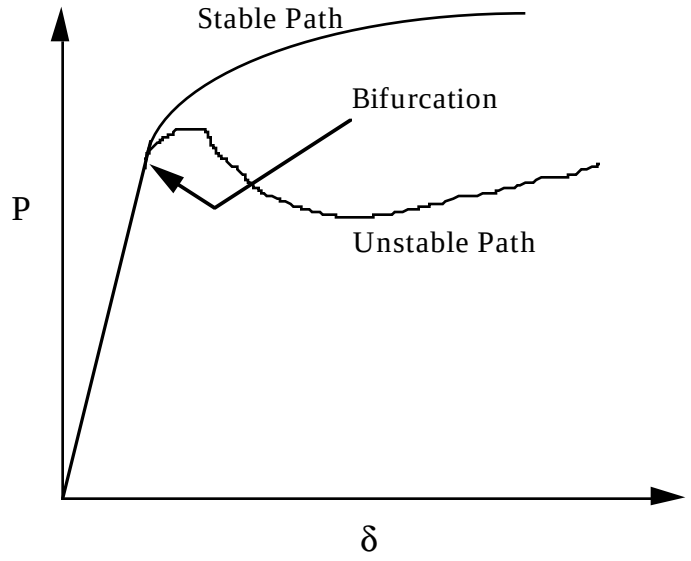

Fig. 3.1 - Load-deflection characteristic of structure showing stable and unstable deformations

The structure’s post-buckling behavior may show a decrease in load carrying capacity with increasing deformation. This type of behavior exhibits an unstable structural response to the applied loads. Furthermore, increasing structural instability may be an indicator of a snap-through condition, where the structure gradually deflects in the direction of the loads with minimal force.

The FEA model is depicted in Fig. 3.2 and 3.3 showing a three-dimensional view of the primary liner. The model comprises a 180° section with symmetry boundary conditions along the X-Y plane. Hydrostatic pressure, corresponding to the different waste levels, is applied as an initial step accounting for the dead loads on the structure. Lastly, external pressure, corresponding to the vacuum load condition, is

applied to the primary liner. The liner boundaries at top and bottom represent locations where displacements and rotations are assumed to be negligible. The upper knuckle tangent conforms to the reinforced concrete dome and is attached to the dome with Nelson studs. The lower knuckle tangent conforms to the refractory concrete below the liner. Therfore, the model is composed primarily of the cylindrical portion of the tank with the upper and lower knuckles.

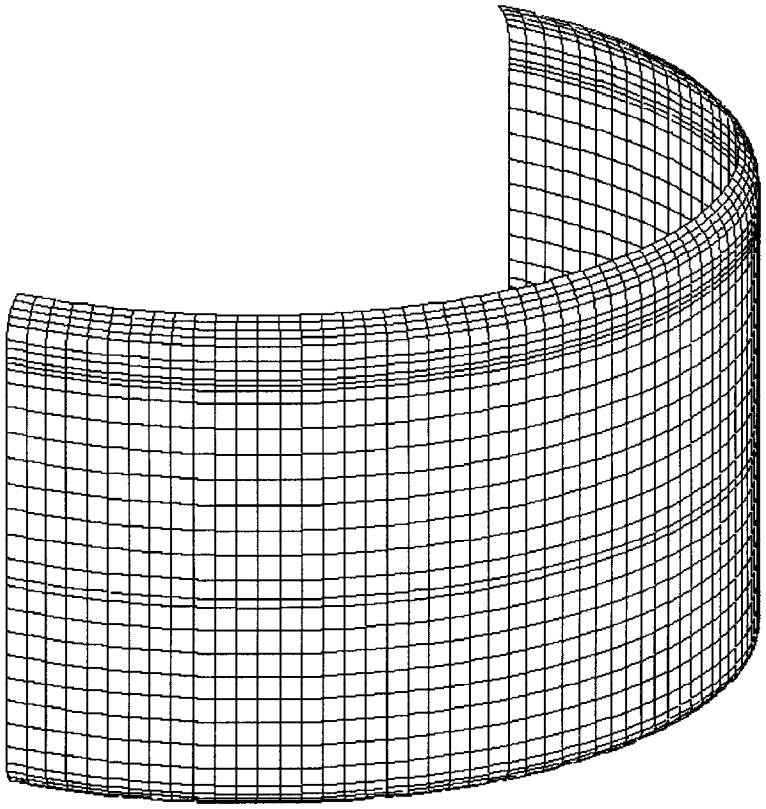

Fig. 3.2. - Finite element model of tank 101-SY for collapse analysis.

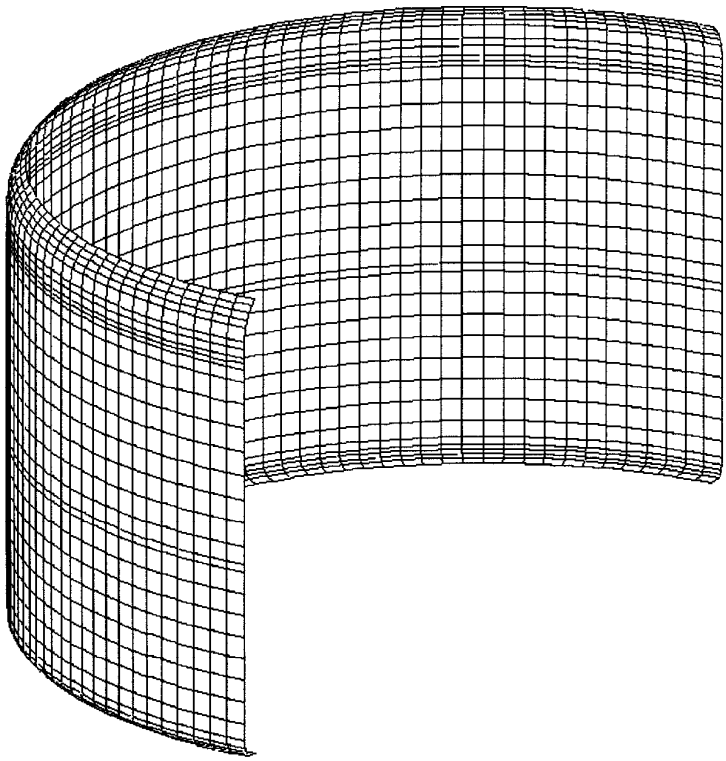

Fig. 3.3. - Finite element model of tank 101-SY for collapse analysis.

Additionally, a final case is evaluated with a fully retrieved tank (empty) having adhered saltcake on the tank walls extending inward and imposing a localized bending moment. This case will determine the reduction in buckling capacity of the tank from the ideal case.

Results of this analysis are compared with a collapse analysis results from WHC[7]. The WHC model included hydrostatic pressure effects for 400” waste level and a specific gravity of 1.0 for the fluid.

4.0 RESULTS

4.1 Theoretical Analysis Results

Classical elastic buckling analysis of unstiffened cylindrical shells shows that tank 101-SY can withstand between 0.6 psig to 1.3 psig. This confirms the original design intent of the tank farm double-shell waste tanks based on design guidance and acceptance criteria of the ASME Code.[1] Attachment 1.0 shows the formulation for buckling capacity as a function of the number of waves developed in the buckled shell.

TABLE 4.1
THEORY vs ASME CODE DESIGN CRITERIA
CRITICAL BUCKLING LOAD COMPARISON

Case	Thickness	Theoretical	ASME Code
1	0.375	0.6	0.78
2	0.500	1.3	1.28

However, since the tank has numerous variations in plate thickness along its height, the above results are merely an estimate of the actual buckling capacity. As will be seen in the following results, the above buckling loads are seen as very good estimates.

4.2 Eigenvalue Buckling Analysis Results

A parametric eigenvalue extraction analysis of the buckling capacity of tank 101-SY was performed with the ABAQUS finite element code[(6)]. Hydrostatic pressure on the tank walls and waste mass effect on tank bottom were varied, representing the different waste levels. The specific gravity of the waste was taken as 1.50 throughout the entire depth of the waste. Under unmitigated tank conditions, there is a marked difference in the density of waste through its depth. However, for this exercise, the density of the waste was taken as constant. The WHC analysis was performed for a waste density of 1.0, representative of H_2O.

Table 4.2 shows the LANL results of the parametric eigenvalue buckling loads for the different waste levels.

TABLE 4.2
EIGENVALUE BUCKLING LOADS VS WASTE LEVEL

Waste Level (in)	Buckling Load (psig)
0	1.678
50	1.688
100	1.702
150	1.753
200	1.904
250	2.241
300	2.826
350	3.830
400	5.715

Results of Table 4.2 are shown graphically in Fig. 4.1.

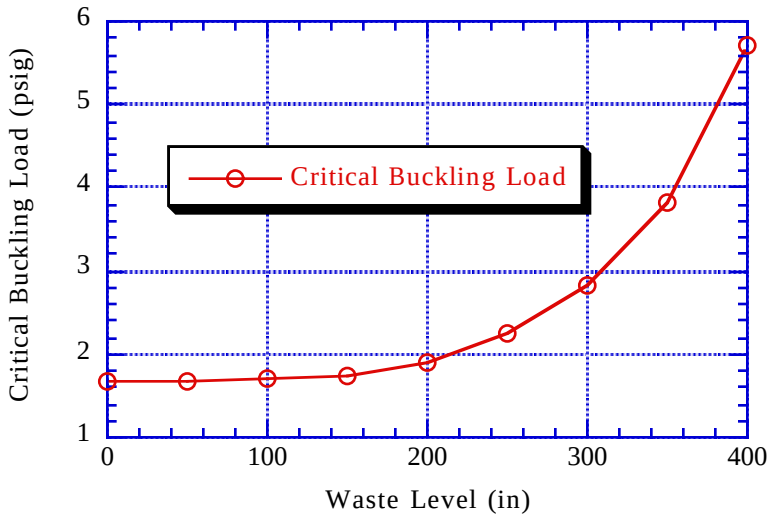

Fig. 4.1 - Critical buckling capacity based on eigenvalue extraction analysis

These results show that the critical buckling pressure as a function of waste level can be described by a 4th-order polynomial:

$$P_{cr} = 1.678 - \left(1.592x10^{-3}\right)L + \left(2.836x10^{-5}\right)L^2 - \left(1.481x10^{-7}\right)L^3 + \left(3.745x10^{-10}\right)L^4 \quad (4.2.1)$$

where; P_{cr} = Critical buckling pressure from eigenvalue analysis, (psig)
L = Waste level, (in)

The critical buckling load for the empty tank is :

P_{cr} = 1.68 psig,

which is equivalent to 46.5" H_2O vacuum pressure. The overall parametric results compare favorably with the WHC results for the buckling capacity of tank 101-SY at a 400" waste level and specific graviy of 1.0 for the waste. The WHC results showed a critical buckling pressure load of 5.8 psig, while the LANL results for the elastic eigenvalue case shows a critical buckling load of 5.7 psig. The reason for the discrepancy is that the LANL analysis solution is based on the elastic eigenvalue extraction while the WHC model used the bifurcation load from the non-linear analysis. The parametric results for the non-linear analyses in Section 4.3 show a much better correleation.

It is important to recognize that for continued waste retrieval operations, there is a reduction in the critical buckling load. For example, a 3.8 psig reduction in buckling capacity is expected in lowering from a 400" waste level to a 200" waste level. The stress stiffening effect of the hydrostatic pressure provides additional capacity against premature buckling.

4.3 Non-Linear Collapse Analysis Results

In order to justify whether the linear buckling analysis truly determined the lowest critical load at a given characteristic mode, a non-linear collapse analysis was performed for the tank primary liner shell. Since a linear eigenvalue analysis may provide a good estimate of the buckling load for a "stiff" structure, it might not predict the collapse (or limit) load quite accurately for structures that may exhibit large displacements, high strains, or an instability. Certain structures that may be considered "imperfection sensitive," will undoubtebly collapse at a lower buckling load than predicted by an eigenvalue analysis. Therefore, non-linear geometric effects and plasticity play an important role in either increasing or decreasing the critical buckling load. External pressure on a cylinder may be considered as an "imperfection starter," since the loads are orthogonal to the structure. As such, a non-linear analysis will provide a better prediction of the limit loads. Lastly, the stability of other possible equilibrium configurations for a particular loading is well predicted by these non-linear effects.

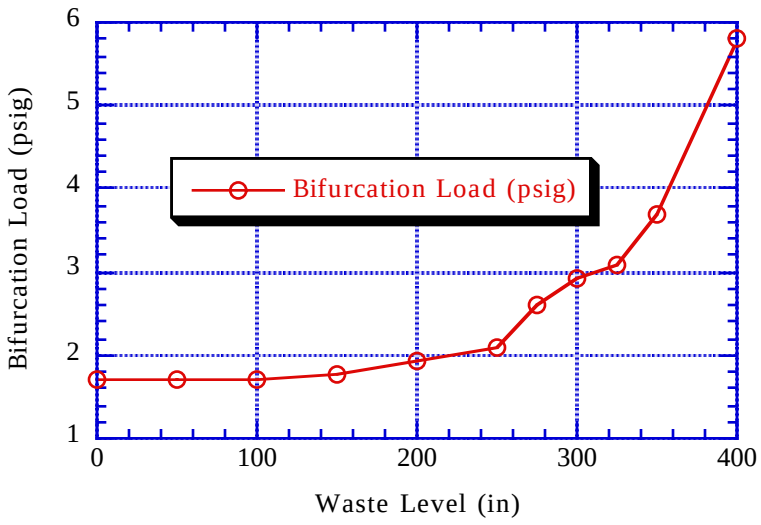

Fig. 4.2 - Bifurcation load vs waste level

The results at a 400" waste level compare favorably with the WHC analysis results, with a few exceptions. As mentioned previously, the WHC analysis used a specific gravity of 1.0 for the waste and half as many elements in the model. The mode shapes are more accurately depicted in the LANL solution because of higher reolution based on a finer mesh. Furthermore, since the bifurcation solution in this model is a classical snap-through problem, the time/load incrementation must be small enough to track the behavior around the sharp curve. The LANL analysis used time/load incrementations of 1/10-th the values used in the WHC analysis. The load-displacement tracking of the snap-through problem is quite evident in several graphical plots shown in the attachments. The above representation can be described by a 4-th order polynomial equation as a function of waste level:

$$P_{bl} = 1.711 + \left(4.346x10^{-3}\right)L - \left(1.153x10^{-4}\right)L^2 + \left(9.581x10^{-7}\right)L^3 - \left(3.018x10^{-9}\right)L^4 + \left(3.586x10^{-12}\right)L^5 \qquad (4.3.1)$$

where: P_{bl} = Bifurcation buckling load from collapse analysis, (psig)
L = Waste level, (in)

TABLE 4.3
COMPARISON OF LINEAR AND NON-LINEAR ANALYSES

Analysis Method	Linear Analysis	Non-Linear Analysis
Waste Level (in)	Eigenvalue Load (psig)	Bifurcation Load (psig)
0	1.678	1.711
50	1.688	1.699
100	1.702	1.707
150	1.753	1.757
200	1.904	1.946
250	2.241	2.095
275	2.447	2.590
300	2.826	2.911
325	3.250	3.091
350	3.830	3.687
400	5.715	5.796

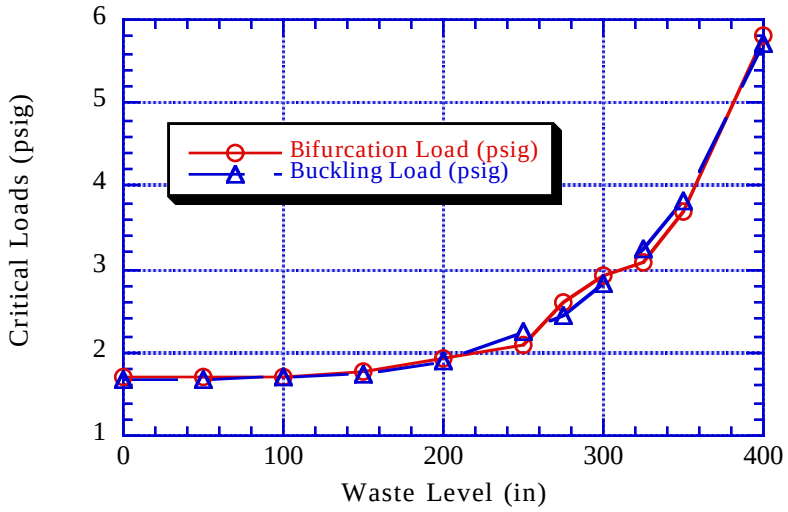

Fig. 4.3 - Eigenvalue buckling load and bifurcation buckling load comparison

5.0 CONCLUSIONS

Hanford HLW Tank 241-SY-101 has been shown to be structurally stable for vacuum loads ranging from 1.68 psig for an empty tank, to 5.72 psig for a waste level of 400-in., based on the lower-bound comparison between the linear elastic eigenvalue buckling analysis and the non-linear finite element model collapse analysis.

The elastic eigenvalue buckling load for the primary liner showed excellent correlation with the bifurcation loads from the non-linear analysis for waste levels of 200-in. and below. For higher waste levels, the linear eigenvalue buckling analysis predicted critical loads slightly lower than the bifurcation loads from the non-linear analysis.

Waste crust assumed adhered to the tank wall reduced the critical buckling load slightly, but the major contributor to the stability of the tank is the vacuum pressure.

It was evident from the non-linear collapse analysis that the structural response of the tank under different waste levels produced a snap-through behavior. Based on the results presented in this report, the critical buckling loads for 101-SY at different waste levels can be represented by the following equation:

$$P_{cr} = 1.678 - \left(1.592x10^{-3}\right)L + \left(2.836x10^{-5}\right)L^2 - \left(1.481x10^{-7}\right)L^3 + \left(3.745x10^{-10}\right)L^4$$

where; P_{cr} = Critical buckling pressure from eigenvalue analysis, (psig)
L = Waste level, (in)

The critical buckling load for the empty tank is :

P_{cr} = 1.68 psig,

6.0 REFERENCES

1. ASME Code, Section VIII, Division 1, "*Pressure Vessels,*" American Society of Mechanical Engineers, (1989)

2. Leach, C. E., Stahl, S. M., "Hanford Site Tank Farm Facilities Interim Safety Basis," Westinghouse Hanford Company, WHC-SD-WM-ISB-001 (August 1993)

3. OSD, "Operating Specifications for the 241-AN, AP, AW, AY, AZ, & SY Tank Farms," Westinghouse Hanford Company, OSD-T-151-00007 (1992)

4. Wood, S. A., "Pressure and Temperature Effects in Tank 101-SY due to Mixing Pump Decontamination Sprays," Westinghouse Hanford Company, Internal Memo 7E880-94-SAW-007

5. Timoshenko, S. P.,"*Theory of Elastic Stability,*" Mc Graw-Hill Book Co., New York, NY (1961)

6. Hibbitt, D., Karlsson, B., and Sorensen, P., "ABAQUS User's Manual," HKS, Inc., Providence, RI (1993)

7. Marlow, R., "Liner Buckling Pressure," Westinghouse Hanford Company, Internal Memorandum CSA:RSM:ggb:94/2, (August 1994)

8. Reynolds, D. A., "101-SY Window C Core Sample Results and Interpretation," Westinghouse Hanford Company report WHC-SD-WM-TI-513, Rev. 0 (1992).

7.0 ATTACHMENTS

7.1 Classical Theoretical Analysis

7.2 Eigenvalue Buckling - ABAQUS Analysis

7.3 Non-Linear Collapse Analysis - ABAQUS Analysis

7.1 Classical Theoretical Analysis

The following calculations are based on classical linear elastic buckling theory for thin cylindrical pressure vessel shells subjected to external pressure. The results will show that the Hanford double-shell tanks have been properly designed for 6" H_2O vacuum. The susceptibility for a cylindrical shell to buckle at a given external pressure (vacuum) is a function of the length-to-radius ratio and the number of waves (or lobes) the buckled shape exhibits.

The critical buckling load is shown by Timoshenko[5] to be the lower-bound of all values of $n = 2,\infty$ for a given cylindrical geometry and thickness. The critical buckling load for a cylindrical pressure vessel is given by :

$$P_{cr} = \frac{Et}{R\left(1-\nu^2\right)}\left[\psi_n + \left(\frac{t^2}{12R^2}\right)\phi_n\right] \qquad (7.1.1)$$

where,

$$\psi_n = \frac{1-\nu^2}{\left(n^2-1\right)\left(1+\frac{n^2L^2}{\pi^2R^2}\right)} \qquad \text{and} \qquad (7.1.2)$$

$$\phi_n = \left(n^2-1\right) + \frac{2n^2-1-\nu}{1+\left(\frac{n^2L^2}{\pi^2R^2}\right)} \qquad (7.1.3)$$

and,

E = Modulus of elasticity, (psi)
t = Shell thickness, (in)
R = Shell radius, (in)
L = Shell length, (in)
ν = Poisson's ratio
n = Number of buckled lobes (waves)

For very long shells where the length-to-radius ratio exceeds about 50, the above equation simply reduces to :

$$P_{cr} = \frac{Et^3}{12R^3}\left(\frac{n^2 - 1}{1 - \nu^2}\right) \qquad (7.1.4)$$

and using $n = 2$, which provides the lowest buckling capacity for very long shells, the critical buckling load becomes:

$$P_{cr} = \frac{Et^3}{4R^3\left(1 - \nu^2\right)} \qquad (7.1.5)$$

However, Tank 101-SY has a length-to-radius ratio of approximately ~1. Therefore, it is evident that the critical buckling load for tank 101-SY will be much higher than for very long shells. Observations of buckled cylindrical shells show that as the shell thickness decreases, (1) the critical load decreases, and (2) the number of lobes at the critical buckling load increase. Secondly, as the length of shell increases, (1) the critical load decreases, and (2) the number of lobes at the critical load decrease.

Assume the tank shell for 101-SY is manufactured completely from 3/8" carbon steel, which should provide the lowest possible estimate of the critical load. Further assume that the tank dome structure provides similar restraints as end-caps on a cylinder, therby giving validity to the above equations. Using the following parameters for the cylindrical portion of the tank shell:

E = 30E+6 psi	R = 450 in.
t = 0.375 in.	L = 410 in.
ν = 0.3	

Then, the critical buckling load is estimated as:

P_{cr} = 0.63 psig

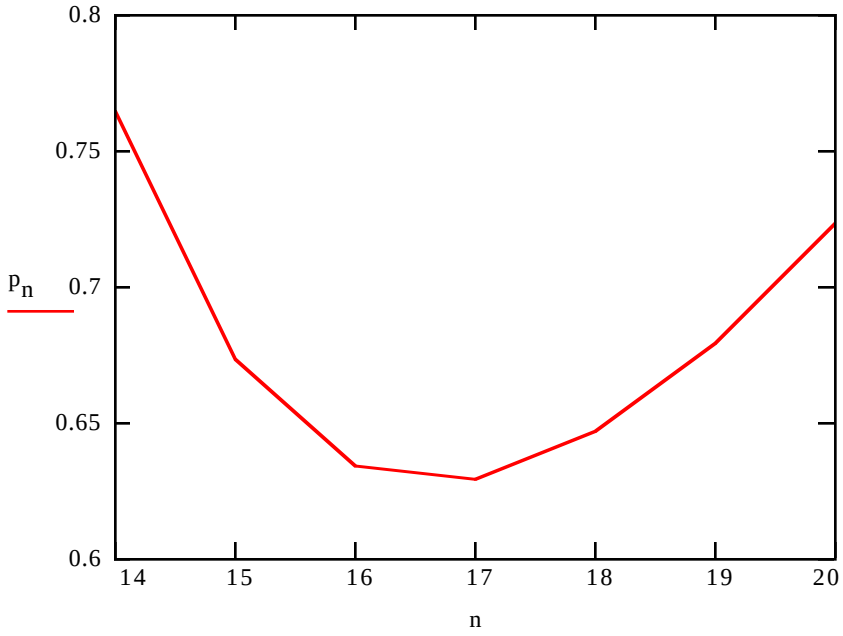

p_n
0.765
0.673
0.635
0.63
0.647
0.679
0.723

Fig. 7.1 - Critical buckling load versus number of lobes, 3/8" shell thickness

Figure 7.1 shows that the lowest buckling load of 0.63 psig is reached with 17 waves (or lobes) circumferentially. Symmetrically placed, these lobes would repeat a pattern on the tank shell every 166 in (~14-ft) in the circumferential direction, or approximately a 21° rotation arc. Since a majority of the tank shell is much thicker than 3/8", including the tank lower knuckle section at 3/4", then the critical buckling load will be somewhat higher than 0.63 psig. If we use a thickness of shell equal to 1/2", the results of Fig. 7.2 show the critical load is:

P_{cr} = 1.3 psig $\qquad\qquad$ n = 16

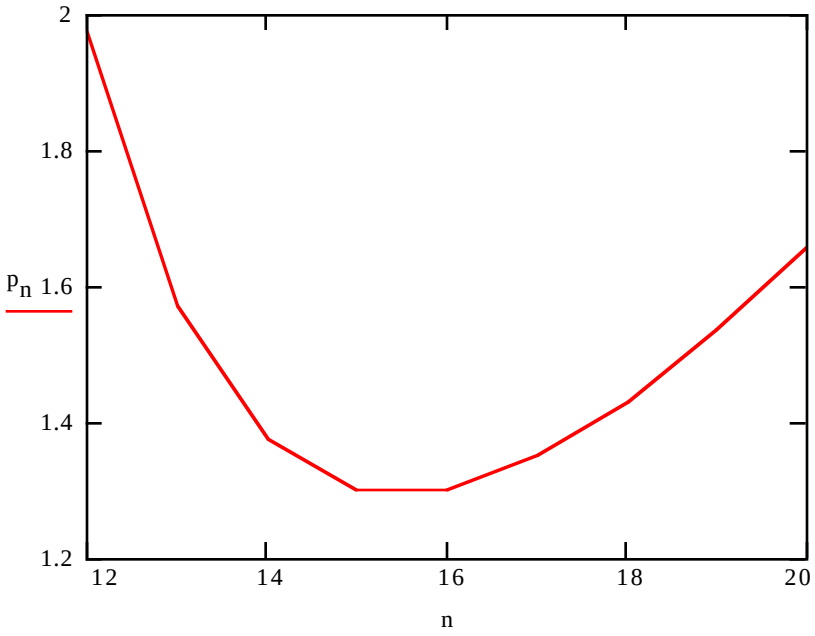

p_n
1.977
1.574
1.378
1.304
1.304
1.352
1.433
1.537
1.66

Fig. 7.2 - Critical buckling load versus number of lobes, 1/2" shell thickness

Based on the results noted above, the linear-elastic critical buckling load for the primary liner is in the range of 0.6 to 1.3 psig, without any safety factors included. The range of critical pressure is dependent on the liner thickness.

Now, let's compare these results to the actual design vacuum pressure of double-shell tanks, based on the ASME Boiler & Pressure Vessel Code requirements. Specifically as a design tool, the ASME code stipulates the design thickness of a cylindrical shell based on the length-to-radius ratio, shell thickness, and modified modulus of elasticity relative to the operating temperature. Furthermore, the Code imposes a safety factor of 3 on the critical buckling load to obtain the maximum allowable working pressure.

The maximum allowable working pressure per the ASME code is derived from the following expression:

$$P_{allow} = \frac{4B}{3\left(\frac{D_o}{t_s}\right)} \qquad (7.1.6)$$

where, D_o = Vessel diameter, (in.)
D_o = 900 in.
t_s = Shell thickness, (in.)
t_s = 0.375 in., and 0.50 in
B = Factor (taken from Fig. 5-UCS-28.2, Sect. VIII, Div. 1)

and, the factor B is a function of the material temperature derived from factor A. Furthermore, A = Factor (taken from Fig. 5-UGO-28.0, Sect. VIII, Div. 1, page 549), where A is based on the diameter-to-thickness ratio and the length-to-diameter ratio of the cylindrical vessel.

TABLE 7.1
ASME CODE ALLOWABLE WORKING PRESSURE
& CRITICAL BUCKLING LOAD

Case	t_s	$\frac{D_o}{t_s}$	A	B	P_{allow}	P_{cr}
1	0.375	2400	3.2E-5	465	0.26	0.78
2	0.50	1800	4.0E-5	575	0.43	1.28

Since the code applies a safety factor of 3.0 to attain the maximum allowable working pressure, the critical buckling load is as shown on the last column. These results compare favorably with the theoretical results noted previously.

TABLE 7.2
THEORY VS ASME CODE DESIGN CRITERIA
CRITICAL BUCKLING LOAD COMPARISON

Case	Thickness	Theoretical	ASME Code
1	0.375	0.6	0.78
2	0.500	1.3	1.28

7.2 Eigenvalue Buckling - ABAQUS Analysis

The finite element formulation method for an eigenvalue buckling analysis is based on the kinematic description of motion of the deforming structure, that includes the constitutive behavior of the specific material models incorporated. This method is strictly beneficial for prediction of critical buckling (or bifurcation) loads for "stiff" structures that exhibit small, elastic deformations, and for which the stress state is well below the yield strength of the material. As stated previously, linear elastic buckling is an eigenvalue extraction solution of the equations describing the deformations, thus allowing a prediction of possible bifurcations associated with kinematic instabilities. The rate-displacement relationship is :

$$\left(\left[K_P\right] + \lambda_i\left[K_Q\right]\right)\{\phi_i\} = dF \qquad (7.2.1)$$

and the eigenvalue problem is the nontrivial solution when $dF = 0$.

$$\left(\left[K_P\right] + \lambda_i\left[K_Q\right]\right)\{\phi_i\} = 0 \qquad (7.2.2)$$

where, K_P = Stiffness matrix of dead loads
K_Q = Stiffness matrix of live loads
λ_i = Eigenvalue of mode i
$\{\phi_i\}$ = Eigenvector matrix

Figures 7.3 through 7.6 show the buckled mode shape of tank 101-SY under vacuum pressure with no internal waste. That is, the hydrostatic effect is not included, which provides additional stress stiffening to the structure. It should be evident from Fig. 7.6 that, although the tank is modeled with a variable thickness, the number of buckled lobes is equivalent to the theoretical prediction.

Figures 7.7 and 7.8 show the buckled mode shape of 101-SY with the waste level modeled at 400-in. The hydrostatic effect of the waste in load stiffening the structure is evident from the buckled lobes above the 400-in level.

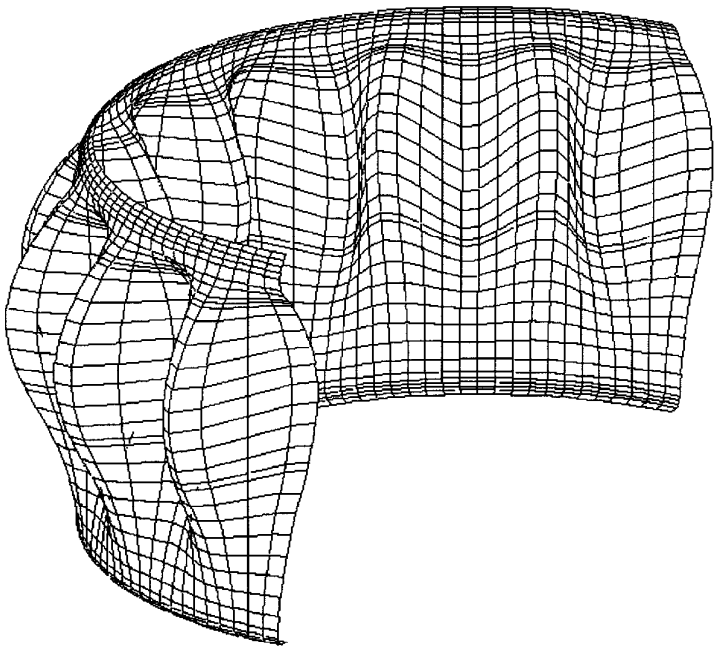

Fig. 7.3 - Buckled mode shape of empty tank.

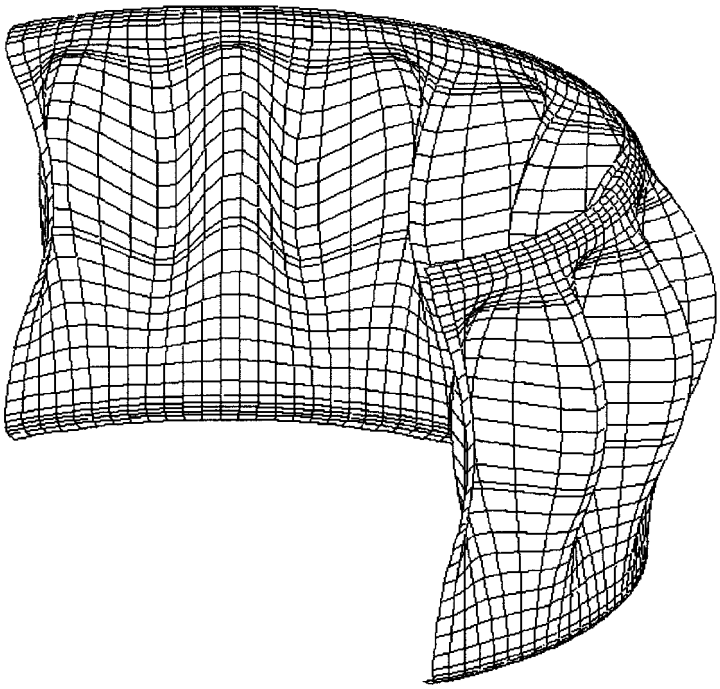

Fig. 7.4 - Buckled mode shape of empty tank.

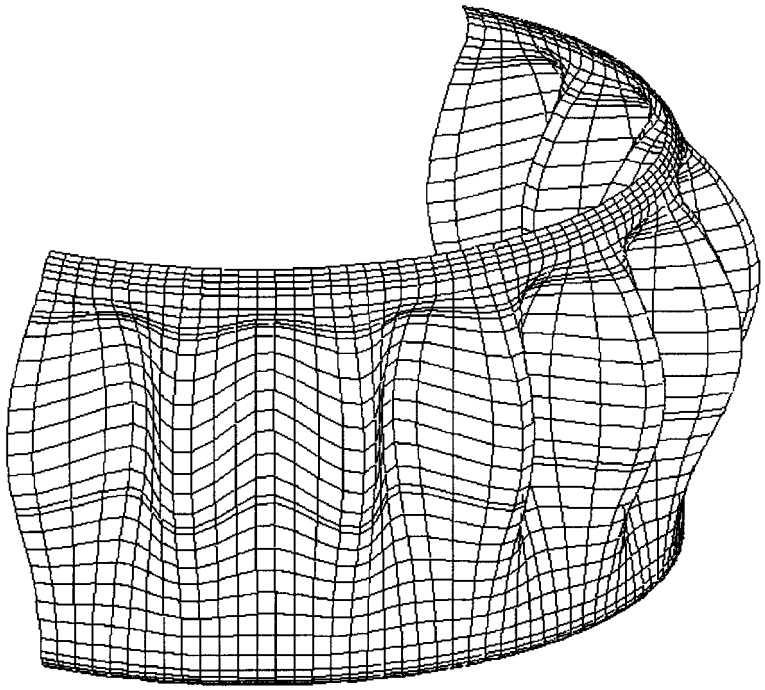

Fig. 7.5 - Buckled mode shape of empty tank.

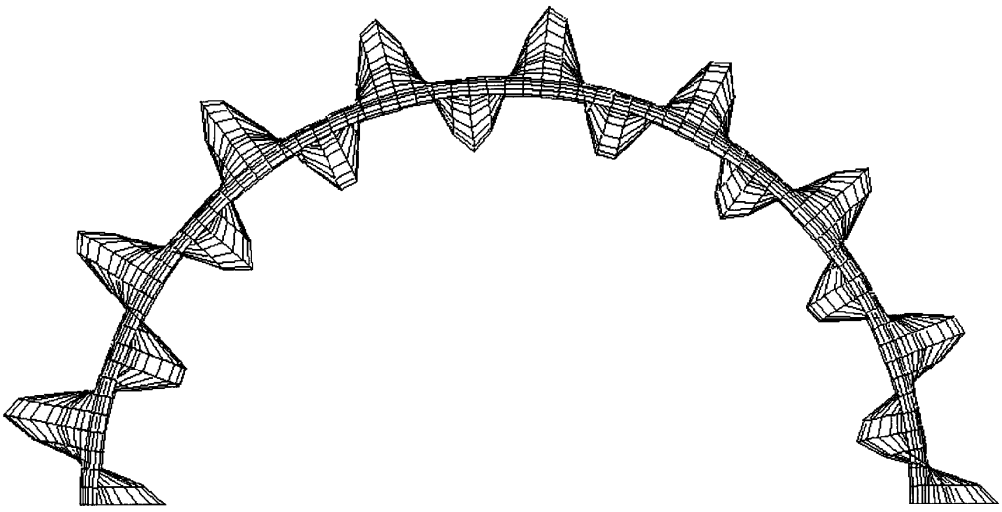

Fig. 7.6 - Buckled mode shape of empty tank (top-down view).

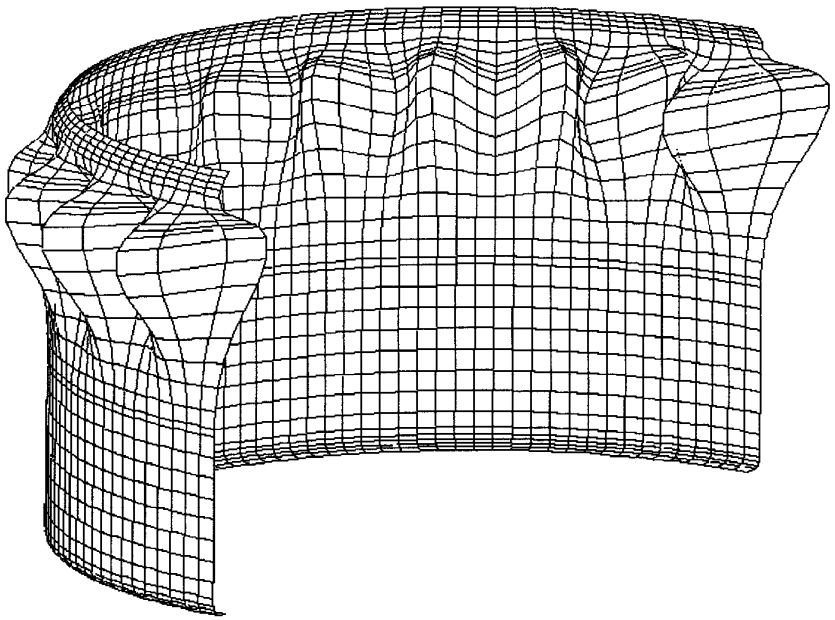

Fig. 7.7 - Buckled mode shape with 400” waste level.

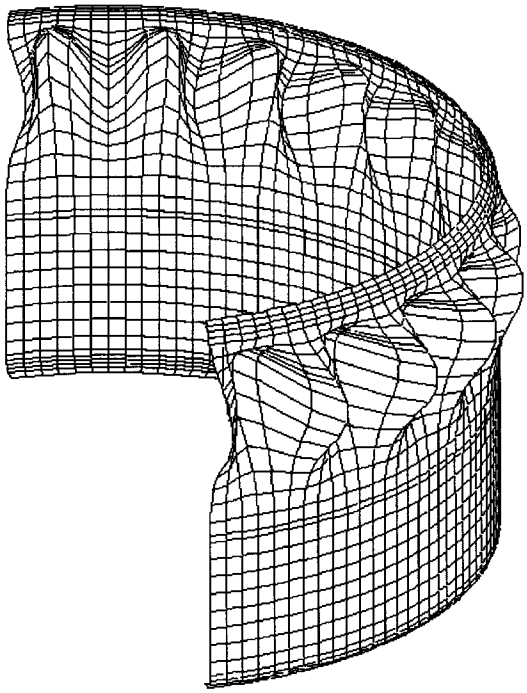

Fig. 7.8 - Buckled mode shape with 400” waste level.

7.3 Non-Linear Collapse Analysis - ABAQUS Analysis

A geometric and material non-linear analysis of the load-deflection characteristic of the structure would undoubtedly be somewhat more accurate in predicting the its response, particularly if the structure attains large deformations and high strains during the loading. Also, imperfection-sensitive structures suffer from

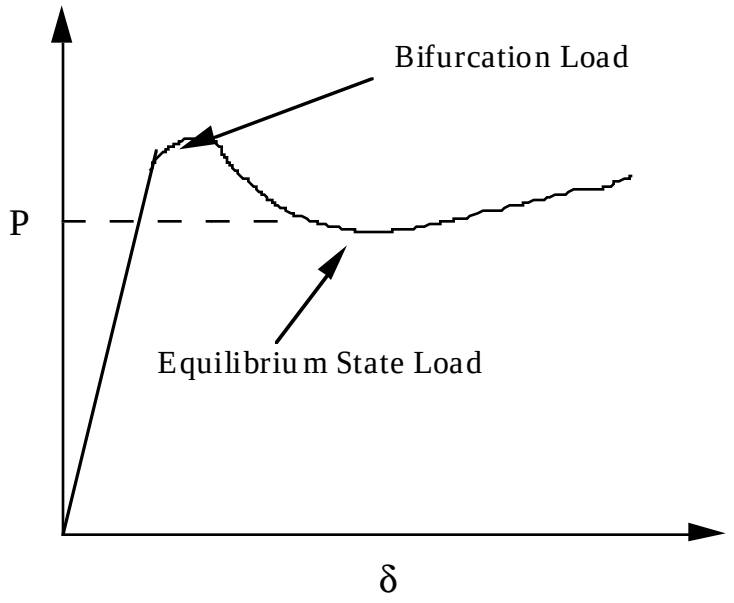

Fig. 7.9 - Load-displacement diagram with unstable response

Results of the non-linear collapse analysis show a distinct structural response at each waste level. It is obvious that, for low waste levels, the effect of waste density, and therefore hydrostatic loads, does not play an important role to the stability of the structure.

At the 400” waste level, we observe a distinct unstable response such that the structure attains an equilibrium load of 1.2 psig, that is slightly lower than the bifurcation load of 1.70 psig (see Fig. 7.10 and 7.11). This is representative of an unstable response indicative of that shown in Fig. 7.9.

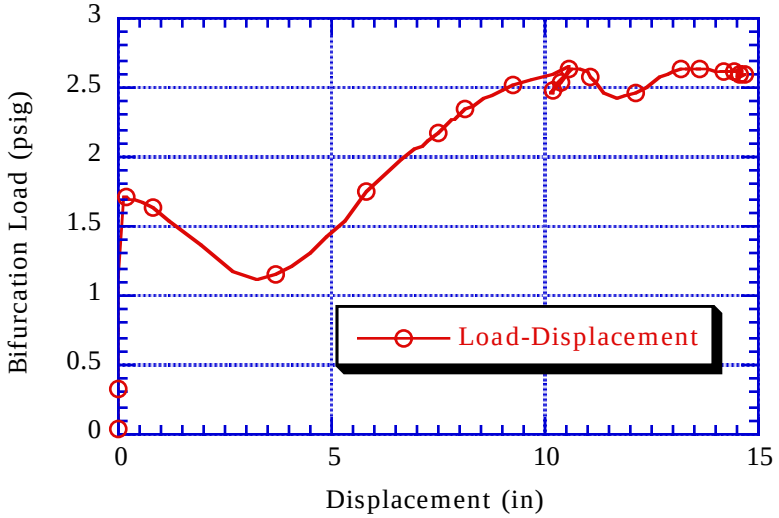

Fig. 7.10 - Post-buckling load for empty tank

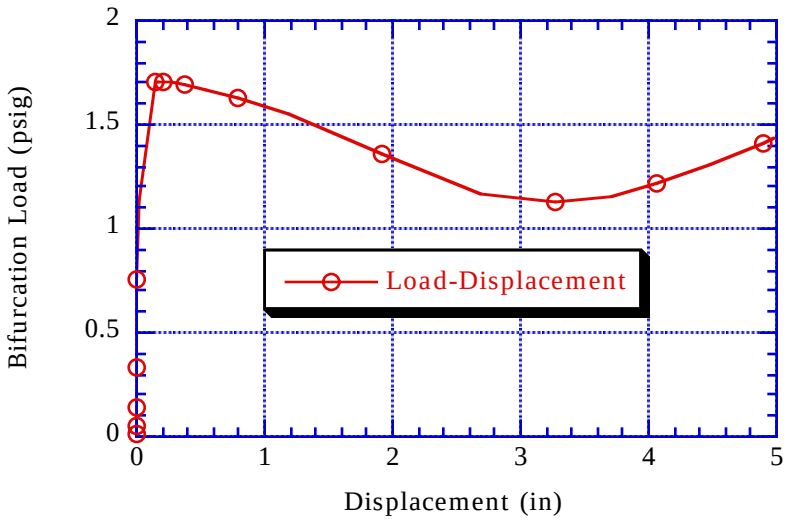

Fig. 7.11 - Post-buckling load for empty tank (zoom plot)

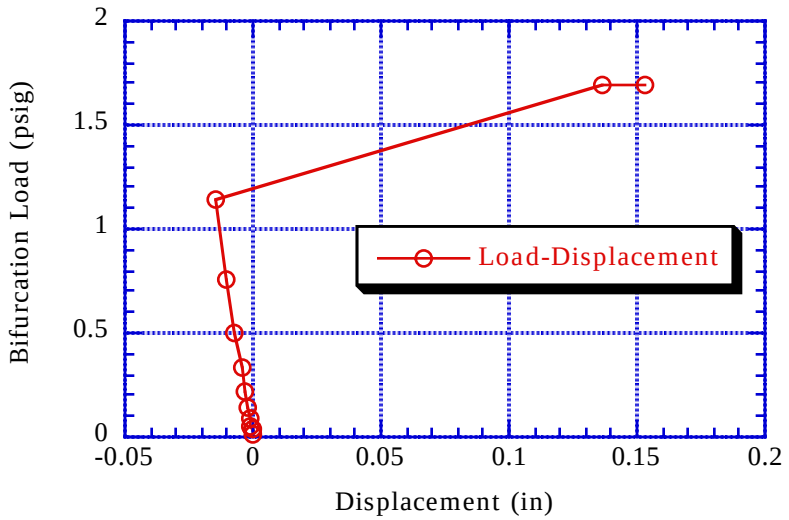

Fig. 7.12 - Post-buckling load for waste level of 50” and specific gravity of 1.50

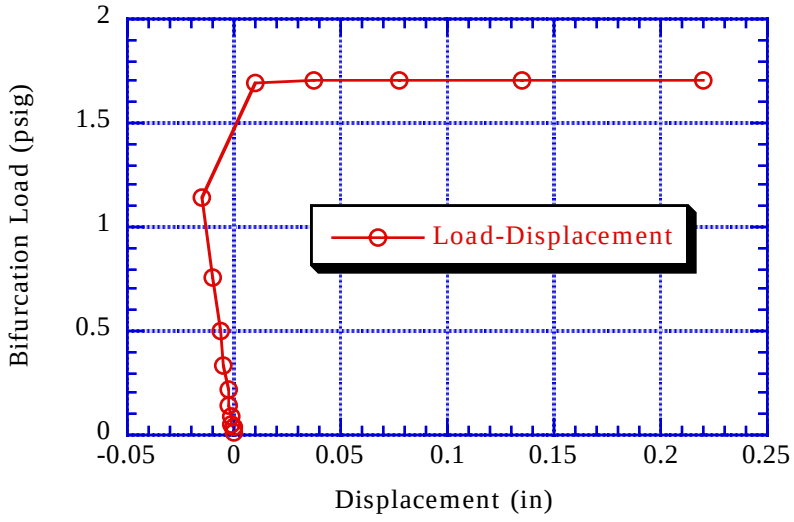

Fig. 7.13 - Post-buckling load for waste level of 100” and specific gravity of 1.50

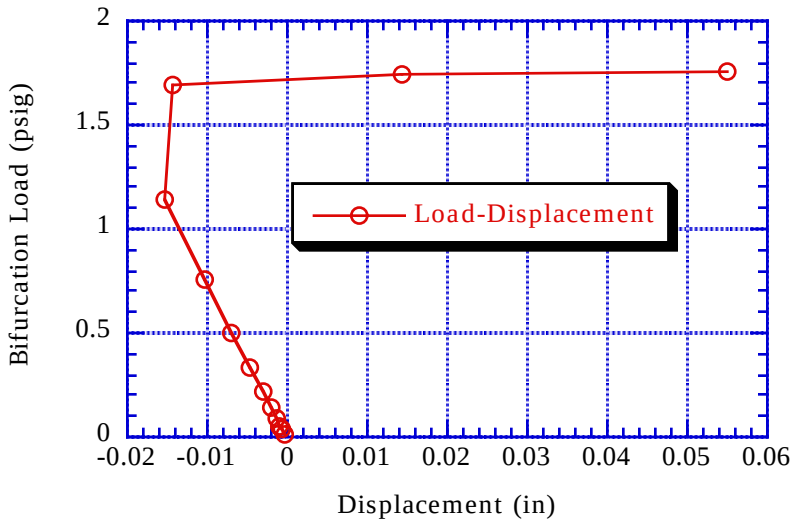

Fig. 7.14 - Post-buckling load for waste level of 150” and specific gravity of 1.50

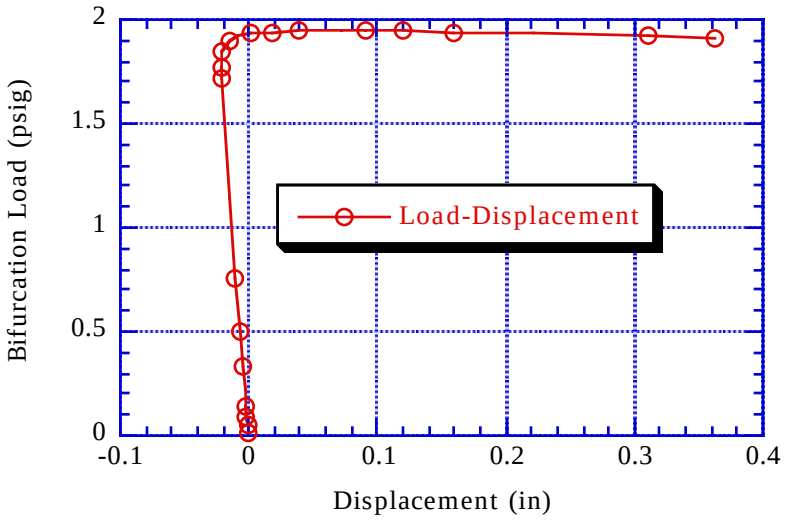

Fig. 7.15 - Post-buckling load for waste level of 200” and specific gravity of 1.50

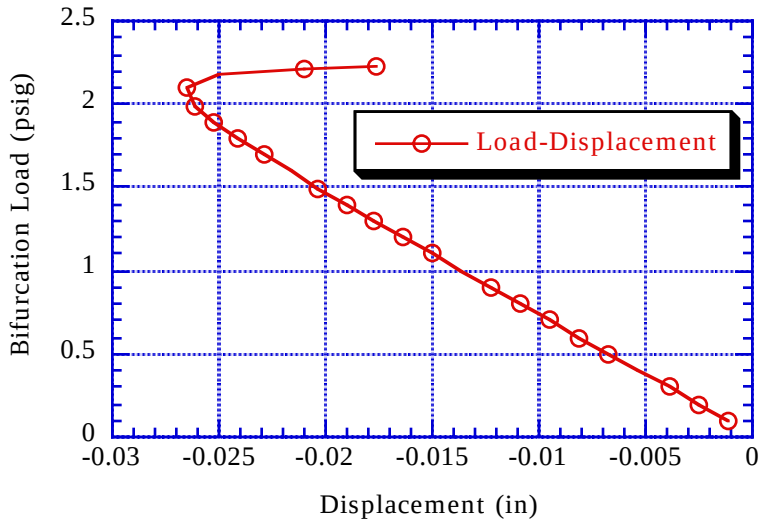

Fig. 7.16 - Post-buckling load for waste level of 250” and specific gravity of 1.50

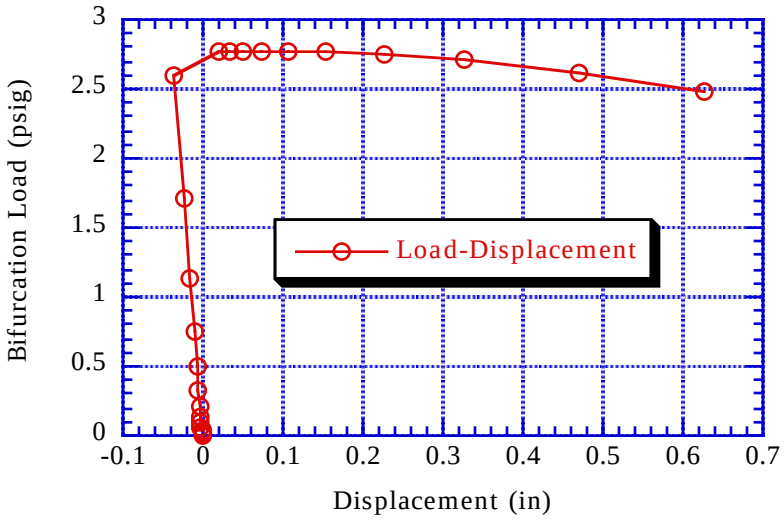

Fig. 7.17 - Post-buckling load for waste level of 275” and specific gravity of 1.50

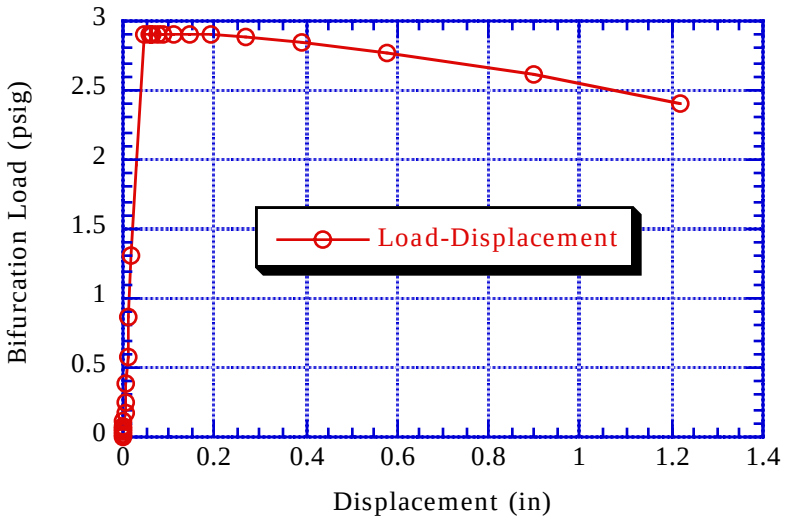

Fig. 7.18 - Post-buckling load for waste level of 300” and specific gravity of 1.50

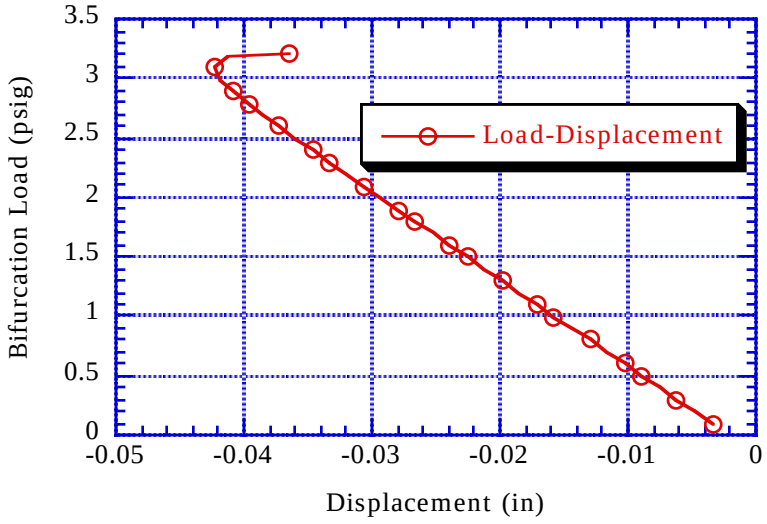

Fig. 7.19 - Post-buckling load for waste level of 325” and specific gravity of 1.50

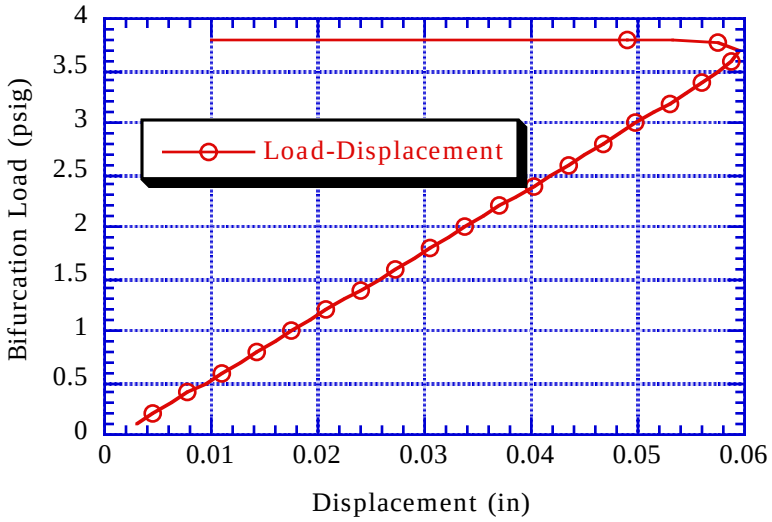

Fig. 7.20 - Post-buckling load for waste level of 350” and specific gravity of 1.50

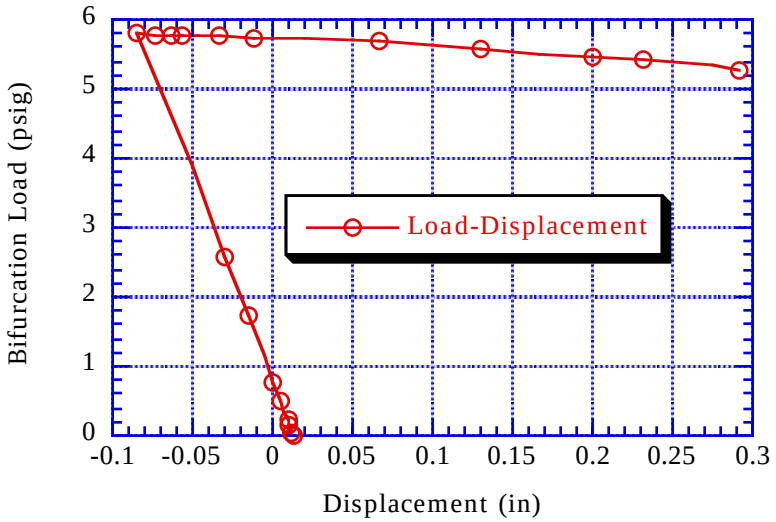

Fig. 7.21 -Post-buckling load for waste level of 400” and specific gravity of 1.50

7.4 Comparison of LANL Results with WHC Analysis Results

Confirmatory analyses were conducted to support the conclusions reached in this report as to the accuracy of the LANL model. The following figures are merely presented to show the comparison with WHC's analysis of Tank 101-SY under a vacuum pressure load and 400" waste level with a specific gravity of 1.0, i.e., representative of water. The refined mesh model used in the LANL analysis produced a better correlation of the tank's response, or buckling mode shape. Furthermore, the time/load incrementation scheme was decreased to one-tenth the initial value used by WHC. This provided a much closer approximation of the bifurcation load at onset of instability. Large time/load increments have a tendency to underpredict or overpredict the actual bifurcation load and subsequent equilibrium positions.

Results ploted in Fig. 7.22 shows the bifurcation load at 5.75 psig with a time-load incrementation of 0.01 sec. The next equilibrium load along the load-displacement path seems to appear around 5.0 psig, while the WHC analysis reported an equilibrium load of 3.4 psig. As mentioned previously, the mesh refinement, coupled with the smaller time-load increments, resulted in closer correlation of the bifurcation load.

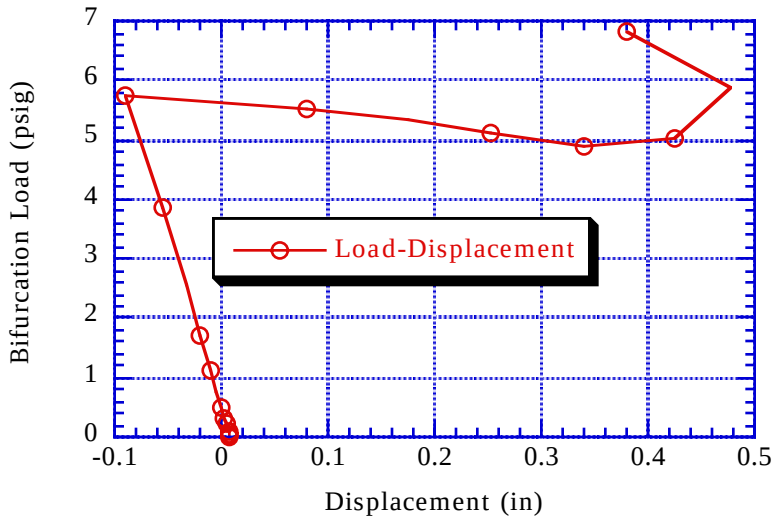

Fig. 7.22 - Critical load for waste level of 400" and specific gravity of 1.0